Field Analysis of Dielectric-Loaded Lens Applicator for Microwave Hyperthermia

Philip H. Alexander, *Member, IEEE,* and Jianfen Liu, *Student Member, IEEE*

Abstract— **A dielectric-loaded waveguide applicator for microwave hyperthermia is analyzed. The phase constant in the waveguide is determined from the numerical solution of the characteristic equation. The field pattern in human muscle which is produced by the applicator is determined by using the Kirchhoff-Huygens principle. The field focusing effect is dependent on the properties of the low permittivity dielectric slab centered in the water-filled waveguide. The greatest field enhancement is found to occur when the slab is 75 mm wide for a 150 mm × 100 mm waveguide at 430 MHz.**

I. Introduction

IT IS THE OBJECTIVE of microwave hyperthermia to produce deep and localized therapeutic heating by electromagnetic waves. Many applicators have been designed for this purpose, e.g. the metal plate lens [1] and the integrated waveguide array [2]. Recently Nikawa *et al.* [3] designed a dielectric-loaded waveguide applicator. Since the field distribution on the aperture can be varied by using different widths of dielectric slab, the applicator is easily fabricated and the resulting penetration depth is controllable. The authors presented the results of experimental measurements of the field values in simulated muscle. It is desirable to have a theoretical analysis of the pattern for such a device. In this paper, the phase constant in the waveguide is calculated directly from the characteristic equation using the Newton-Raphson method. The near field pattern inside the human muscle is obtained using the Kirchhoff-Huygens principle.

II. The Phase Constant of the Dielectric-Loaded Waveguide

A dielectric-loaded waveguide can be utilized as a phase shifter or an impedance matching section [4]. The geometry and coordinate system are shown in Fig. 1 where a dielectric slab (ϵ_2) is shown centered in the water-filled (ϵ_1) waveguide. The general nature of the field distribution over the aperture is shown in Fig. 2. The maximum field is always located in the higher dielectric constant region. To achieve focusing, ϵ_1 should be much greater than ϵ_2. According to [3], $\epsilon_1 = 78$ (pure water) and $\epsilon_2 = 2.3$ (polyethylene) at 430 MHz with a waveguide dimension $a = 150$ mm and $b = 100$ mm. Considering the boundary conditions and assuming no y dependence, the field in the three regions can be expressed as:

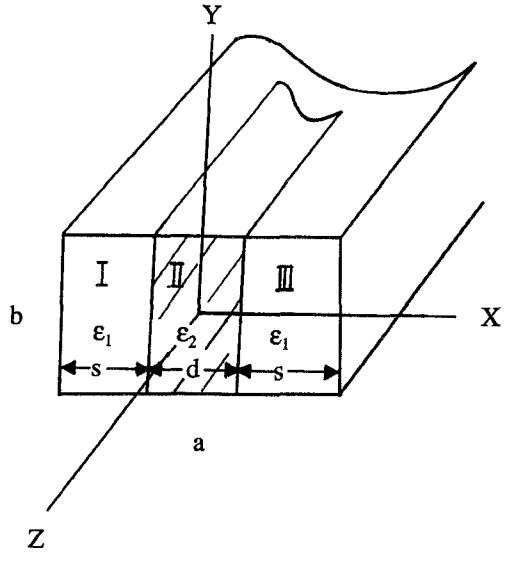

Fig. 1. The geometry of a dielectric-loaded waveguide.

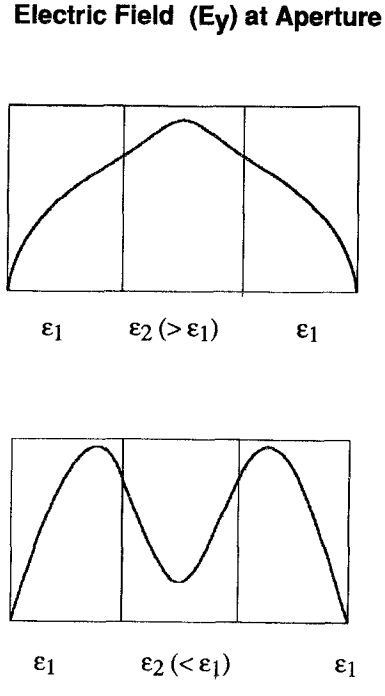

Fig. 2. General field distribution on the aperture. (a) $\epsilon_1 < \epsilon_2$ (b) $\epsilon_1 > \epsilon_2$.

in region I and III, when $k_{x1} = jh$

$$H_z = A \cos\left[h\left(\frac{a}{2} - |x|\right)\right]$$

Manuscript received June 1, 1992; revised September 21, 1992.

The authors are with the Department of Electrical Engineering, University of Windsor, Windsor, Ontario, Canada N9B 3P4.

IEEE Log Number 9207406.

$$H_x = A\frac{j\beta}{h}\sin\left[h\left(\frac{a}{2}-|x|\right)\right]$$
$$E_y = -A\frac{j\omega\mu}{h}\sin\left[h\left(\frac{a}{2}-|x|\right)\right]; \quad (1)$$

in region II, when $k_{x2} = l$

$$H_z = B\sinh(lx)$$
$$H_x = -B\frac{j\beta}{l}\cosh(lx)$$
$$E_y = B\frac{j\omega\mu}{l}\cosh(lx); \quad (2)$$

or in region II, when $k_{x2} = jl$

$$H_z = B\sin(lx)$$
$$H_x = B\frac{j\beta}{l}\cos(lx)$$
$$E_y = -B\frac{j\omega\mu}{l}\cos(lx); \quad (2a)$$

where A, B are proportionality constants, k_{x1} and k_{x2} are the differential equation separation constants (which are expanded in terms of h and l in (1) and (2)) in dielectric region I and II respectively, and β is the phase constant in the waveguide. Using the boundary conditions that H_z and E_y are continuous at interface $x = d/2$,

$$\begin{aligned} A\cos(hs) - B\sinh(ld/2) &= 0. \\ A\sin(hs)/h + B\cosh(ld/2)/l &= 0. \end{aligned} \quad \text{when } k_{x2} = l \quad (3)$$

$$\begin{aligned} A\cos(hs) - B\sin(ld/2) &= 0. \\ A\sin(hs)/h - B\cos(ld/2)/l &= 0. \end{aligned} \quad \text{when } k_{x2} = jl \quad (3a)$$

The characteristic equation is

$$\tan(hs)/h = -\coth(ld/2)/l \qquad \text{when } k_{x2} = l \quad (4)$$

or

$$\tan(hs)/h = \cot(ld/2)/l \qquad \text{when } k_{x2} = jl \quad (4a)$$

Equation (4) or (4a) together with the following two equations give the separation constants h, l and the phase constant β. The differential equation applied to the two regions yields

$$h^2 + \beta^2 = \omega^2\mu_o\epsilon_1\epsilon_o, \quad (5a)$$
$$\beta^2 - l^2 = \omega^2\mu_o\epsilon_2\epsilon_o, \qquad \text{when } k_{x2} = l \quad (5b)$$
$$\beta^2 + l^2 = \omega^2\mu_o\epsilon_2\epsilon_o, \qquad \text{when } k_{x2} = jl \quad (5c)$$

where μ_o and ϵ_o are the permeability and permittivity in free space respectively. Transcendental equation (4) or (4a) can be solved using the Newton-Raphson method [5] with (5). The proportionality constant B is then determined from (3) or (3a)'. Usually there are multiple solutions for h, l and β. The lowest value of h and l gives the dominant mode; other values of h, l are associated with higher order modes. Table I lists the solutions for h, l and β for different slab widths. Table I(a) shows the dominant propagation mode. The solutions in Table I(b) are for the second mode. Since the phase constant is pure imaginary, these modes are not propagating. The field strength decays as $\exp(-|\beta|z)$ along the z direction. Parameters for higher order modes are not shown since they attenuate very rapidly with increasing z and would not be significant in amplitude at the aperture.

TABLE I
SOLUTIONS FOR h, l AND β IN DIELECTRIC -LOADED WAVEGUIDE

(a) Dominant Mode (Eq. (4), 5(a) and 5(b))			
d (mm)	h (m^{-1})	l (m^{-1})	β (m^{-1})
30	41.06	66.78	68.16
45	46.63	63.02	64.48
60	52.76	57.98	59.57
75	60.00	50.45	52.27
90	68.43	38.24	40.61
105	—	—	—
(b) Higher Order (evanescent) Mode (Eq. (4), 5(a) and 5(c))			
d (mm)	h (m^{-1})	l (m^{-1})	β (m^{-1})
30	316.15	306.28	$j305.97$
45	112.96	81.34	$j80.18$
60	115.21	84.43	$j83.32$
75	318.88	309.10	$j308.79$
90	197.96	181.67	$j181.15$
105	161.52	141.23	$j140.56$

TABLE II
ELECTRIC FIELD PEAK VALUES ON THE APERTURE AT VARIOUS d/a VALUES

d/a	peak* (dB)	$x/(a/2)$
0.2	8.0	0.48
0.3	10.6	0.55
0.4	12.5	0.60
0.5	12.8	0.64
0.6	10.3	0.71

Relative to the values at the center of the aperture

Nikawa *et al.* [3] used the approximation formula for β which is obtained from the variation method as presented by Berk [6]. This method used $E_y = \sin(\pi x/a)$ as a trial field and is only applicable for the case when ϵ_1 and ϵ_2 are not much different or when d/a is very small. For the dielectric ratio $\epsilon_1/\epsilon_2 = 34$ (the present condition), this variation method is hardly applicable as shown in Fig. 3, where h, l, β are the precise numerical results from Table I(a), h', l' and β' are the results according to the method by Nikawa *et al.* [3]. Actually the approximation is only good for $d/a \leq 0.05$.

The phase constant decreases with the increase of d/a. After $d/a \approx 0.7$, the wave will not propagate in the waveguide. When a wave is close to cutoff, wall loss becomes severe, so we impose the restriction $d/a \leq 0.7$ and assume the presence of the dominant mode only at the aperture in the following analysis.

The field distribution on the aperture for different d/a values is shown in Fig. 4. There are two peaks in the higher permittivity regions and they act to enhance the field on the z axis. The peak values relative to the field at the center of the aperture are shown in Table II. The peak value increases with d/a initially, reaches a maximum of 12.8 dB near $d/a = 0.5$, then decreases with further increase of d/a. Because the

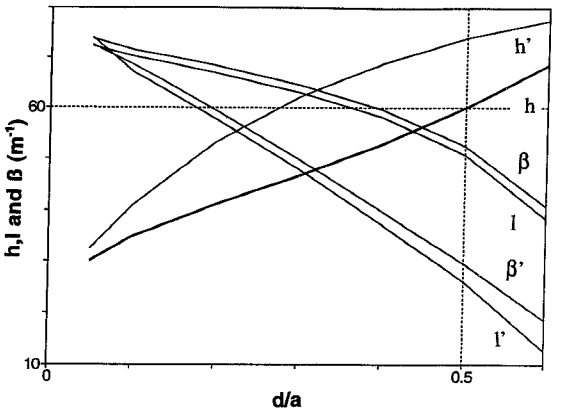

Fig. 3. The separation constants h, l and β as a function of slab width. h, l, β numerical results from transcendental equation. h', l', β' results from the method by [3].

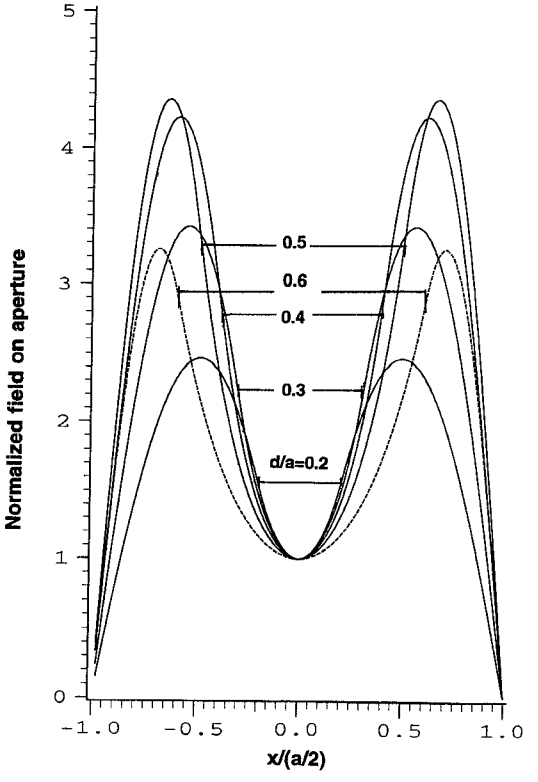

Fig. 4. Field distribution on aperture with different slab widths. The horizontal lines represent the slab widths.

focusing effect on the z axis depends on this peak value, better focusing is expected for slab widths d in the range $0.4 \leq d/a \leq 0.6$. Table II also shows that the peak positions move outward as d/a increases.

III. The Field Pattern Inside Human Muscle

The electric field at an observation point (x, y, z) due to the dielectric-loaded waveguide applicator is calculated according to the Kirchhoff-Huygens principle [7] from

$$\boldsymbol{E}(x,y,z) = -\frac{1}{4\pi}\iint_S [j\omega\mu(\boldsymbol{n}\times\boldsymbol{H})G + (\boldsymbol{n}\times\boldsymbol{E}) \times \nabla G + (\boldsymbol{n}\cdot\boldsymbol{E})\nabla G]\, ds$$

TABLE III
Attenuation and Phase Constant in Human Muscle

ϵ'	ϵ	k (m^{-1})	α (m^{-1})
79	35	82.30	17.26
		(82.30)	(10.00)
57	36	71.08	20.50

where the Green's function

$$G = \frac{\exp[-(\alpha+jk)R]}{R},$$
$$R = \sqrt{[(x-x')^2 + (y-y')^2 + (z-z')^2]}, \qquad (7)$$

$\boldsymbol{n} = \boldsymbol{z}, (x', y', z')$ is the source integration point, α and k are the attenuation and phase constant in human muscle respectively, and the integration is taken over the aperture S. Collin's analysis of dielectric-slab-loaded rectangular guides [8] indicates that there is no axial electric field component present. Therefore we assume that there is no normal electric field component on the aperture, $\boldsymbol{n}\cdot\boldsymbol{E} = 0.$, and the field components inside human muscle are

$$E_y(x,y,z) = -\frac{1}{4\pi}\iint_S E_y(x')\frac{\exp[-(\alpha+jk)R]}{R^2} \cdot\left[-(\alpha+jk)z - \frac{z}{R}\right]dx'\,dy' - \frac{1}{4\pi}\iint_S j\omega\mu H_x(x') \cdot\frac{\exp[-(\alpha+jk)R]}{R}dx'\,dy' \qquad (8)$$

$$E_z(x,y,z) = \frac{1}{4\pi}\iint_S E_y(x')\frac{\exp[-(\alpha+jk)R]}{R} \cdot\left[-(\alpha+jk)(y-y') - \frac{y-y'}{R}\right]dx'\,dy' \qquad (9)$$

where $E_y(x')$ and $H_x(x')$ are assumed to be the fields on the aperture from (1) and (2). The complex relative permittivity of human muscle is taken as $79 - j35$ (at 400 MHz, 29.5°C [2]). In [2], the authors used a 0.2 percent saline solution as a simulator of muscle and fat, while in [3], they used a 0.4 percent saline solution (the permittivity was not specified). From measurement [9], the complex dielectric constant of muscle is $57 - j36$ (at 500 MHz, 25°C). The present calculation is performed for both values for comparison. The attenuation and phase constant are calculated according to

$$k^2 - \alpha^2 = \omega^2\mu_o\epsilon'\epsilon_o$$
$$2\alpha k = \omega^2\mu_o\epsilon''\epsilon_o. \qquad (10)$$

The results are shown in Table III. The α and k values in parentheses are also used in calculation to show the effect of dielectric loss.

The electric field distribution in human muscle with a dielectric constant $79 - j35$ is shown in Fig. 5 with a slab width $d/a = 0.4$. The field enhancement effect on the z axis is due to the presence of the two peaks in the transverse amplitude distribution. The higher the peaks, the more pronounced the effect.

TABLE IV
MAXIMUM FIELD AND POSITION IN HUMAN MUSCLE AT DIFFERENT d/a VALUES

	$k = 82.3$	$\alpha =$ 17.26	$k = 82.3$	$\alpha =$ 10.0	$k =$ 71.08	$\alpha =$ 20.56
d/a	Max (dB)	z (mm)	Max (dB)	z (mm)	Max (dB)	z (mm)
0.2	1.20	20	2.67	25	0.21	10
0.3	2.35	25	4.09	30	0.68	15
0.4	3.44	25	5.46	35	1.12	20
0.5	4.02	30	6.65	40	1.26	20
0.6	2.09	30	5.43	40	0.31	15

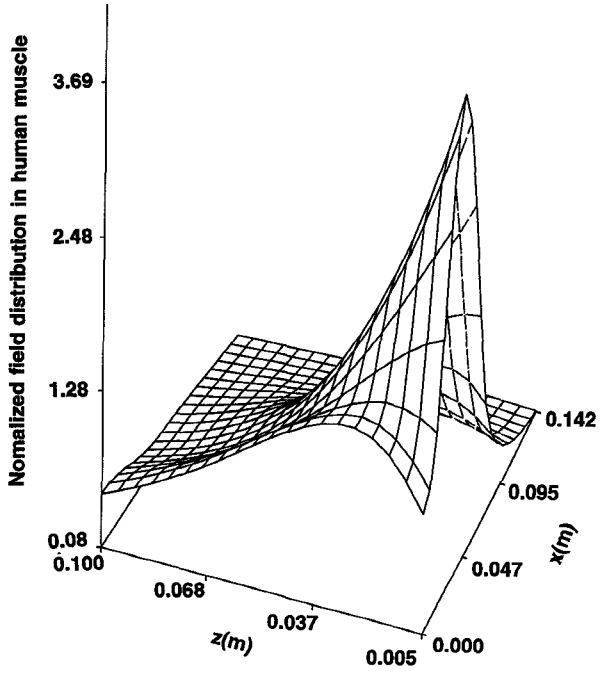

Fig. 5. 3-D field pattern in human muscle, $\epsilon' - j\epsilon = 79 - j35, d/a = 0.4$.

It is more convenient to show the field on the z axis as in Fig. 6. With increasing d/a, the maximum field on the z axis varies from 1.2 dB ($d/a = 0.2$) through a maximum of 4 dB ($d/a = 0.5$) and then decreases. Table IV shows the maximum field and position for various slab widths. The maximum field position is 30 mm from the aperture when $d/a = 0.5$. The greatest penetration depth is 91 mm. The penetration depth is defined as the depth at which the field decreases by 3 dB from the level at the center of the aperture.

Fig. 7 shows the field along the z axis when the medium is less lossy ($\alpha = 10\,\mathrm{m}^{-1}, k = 82.3\,\mathrm{m}^{-1}$). The maximum field can be 6.65 dB and the maximum field position is 40 mm from the aperture when $d/a = 0.5$. Fig. 8 shows the field in a more lossy medium with $\epsilon' - j\epsilon = 57 - j36\,(\alpha = 20.56\,\mathrm{m}^{-1}, k = 71.08\,\mathrm{m}^{-1})$. The maximum field is only 1.26 dB; the maximum field position is 20 mm and the penetration depth is 60 mm.

From Table IV, the focusing effect and maximum position are dependent on the width of the dielectric slab and the dielectric properties of the target media. The largest field enhancement is achieved at $d/a = 0.5$ for the three sets of dielectric constant in Table III. Nikawa *et al.* [3] found that $d/a = 0.6\,(d = 90$ mm) results in the best focussing effect for a 0.4 percent saline solution. The difference may be caused by the following factors: a) different dielectric constant value; b) the possible existence of higher order modes in the measurement system.

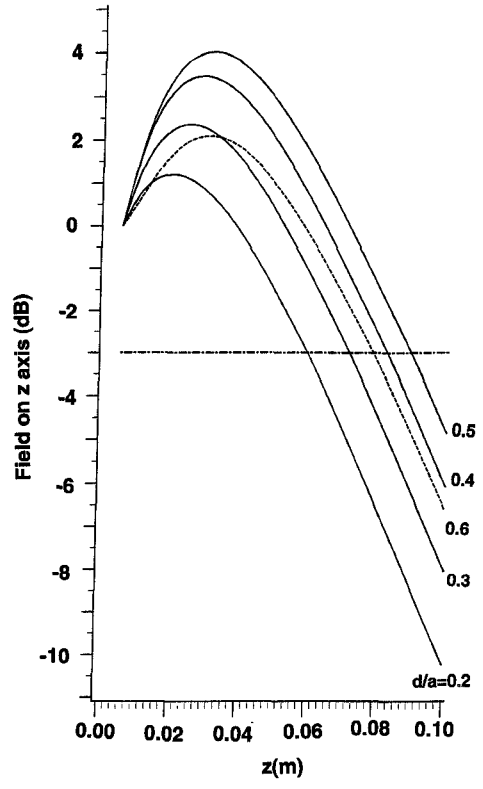

Fig. 6. Field on z axis at different d/a values in human muscle with $k = 82.3\,(\mathrm{m}^{-1}), \alpha = 17.26\,(\mathrm{m}^{-1})$.

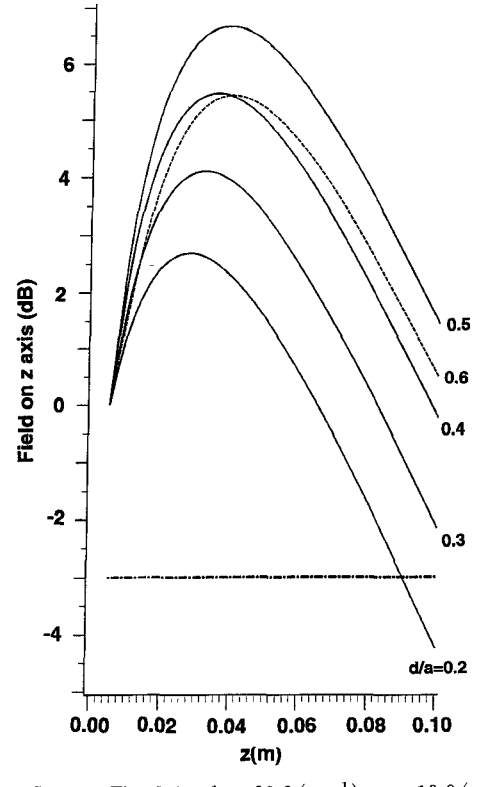

Fig. 7. Same as Fig. 6, but $k = 82.3\,(\mathrm{m}^{-1}), \alpha = 10.0\,(\mathrm{m}^{-1})$.

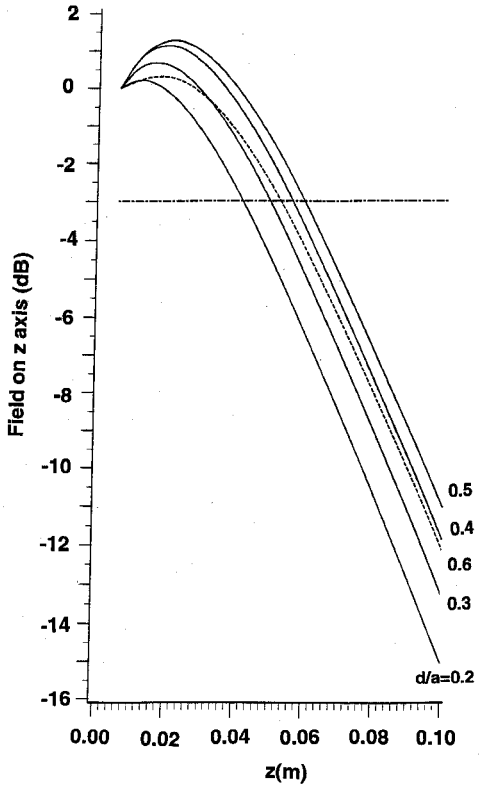

Fig. 8. Same as Fig. 6, but $k = 71.08\,(\mathrm{m}^{-1}), \alpha = 20.56\,(\mathrm{m}^{-1})$.

Reference [3] did not provide the value of the complex dielectric constant for the 0.4 percent saline solution. The measurements in [3] show that there was a variation in the phase of the field over the illuminating aperture. This is the evidence of the presence of one or more nonnegligible higher order mode fields at that location. Although full details of the physical construction of the taper and dielectric-loaded waveguide section leading to the aperture was not provided, it appears that some degree of discontinuity in the waveguide walls is introduced by the water inlet and outlet orifices. These are located a small distance (apparently the length of the slab) behind the aperture. The relative amplitude and phase of higher order modes can only be obtained when the precise excitation field and the length of the dielectric-loaded waveguide are provided. Since [3] did not provide these details, exact agreement between the present calculation and the experiments can not be expected.

IV. Conclusion

The dielectric-loaded waveguide can be used as an applicator for microwave hyperthermia at 430 MHz. It is found that the phase constant in the waveguide presented in [3] is not appropriate for the measurement conditions cited. The characteristic equation was solved here for the phase constant in the dielectric-slab-loaded waveguide for conditions associated with the geometry of the proposed applicator. The best focusing effect can be achieved when the slab is 75 mm wide in a 150 mm × 100 mm waveguide at 430 MHz.

Differences from experimentally determined optimum conditions appear to be due to the presence of one or two higher order modes in the experimental set-up, and to the fact that the dielectric parameters of the target medium were not specified for the system measured.

References

[1] Y. Nikawa, M. Kikuchi, and S. Mori, "Development and testing of a 2450 MHz lens applicator for localized microwave hyperthermia," *IEEE Trans. Microwave Theory Tech.*, vol. MTT-30, pp. 1212–1216, Nov. 1985.

[2] Y. Nikawa, T. Katsumata, M. Kikuchi, and S. Mori, "An electric field converging applicator with heating pattern controller for microwave hyperthermia," *IEEE Trans. Microwave Theory Tech.*, vol. MTT-34, pp. 631–635, 1986.

[3] Y. Nikawa and F. Okada, "Dielectric-loaded lens applicator for microwave hyperthermia," *IEEE Trans. Microwave Theory Tech.*, vol. 39, pp. 1173–1178, 1991.

[4] G. N. Tsandoulas, D. H. Temme, and F. G. Willwerth, "Longitudinal section mode analysis of dielectric-loaded rectangular waveguides with application to phase shifter design," *IEEE Trans. Microwave Theory Tech.*, vol. MTT-18, pp. 88–95, 1970.

[5] S. G. Kellison, *Fundamentals of Numerical Analysis*. Richard D. Irwin, Inc., 1975, pp. 263–267.

[6] A. D. Berk, "Variational principle for electromagnetic resonators and waveguide," *IRE-4*, no. 2, pp. 104–110, 1956.

[7] J. A. Stratton, *Electromagnetic Theory*. New York: McGraw-Hill, 1941, pp. 460–470.

[8] R. E. Collin, *Field Theory of Guided Waves*. New York: McGraw-Hill, Sec. 6.1, 1960, pp. 224–225.

[9] M. A. Stuchly and S. S. Stuchly, "Dielectric properties of biological substances - tabulated," *J. Microwave Power*, vol. 15, pp. 19–26, 1980.

Philip H. Alexander (S'65–M'66) was born in Windsor, Ontario, Canada. He received his Bachelor of Applied Science degree from Assumption University, Windsor, Ontario in 1963 and his Master of Applied Science degree from the University of Windsor, Windsor, ONT in 1964, both in Electrical Engineering.

He has pursued further graduate work at the University of Michigan, Ann Arbor, MI where he was employed in the Cooley Electronics Laboratory from 1970 to 1972. He is now an Associate Professor in the Electrical Engineering Department of the University of Windsor where he has been teaching since his initial appointment in 1964. He has served as the Assistant to the Dean of Engineering and as the Head of the Electrical Engineering Department. He has been active in research and consulting work involving electromagnetic modelling of electric power distribution components and microwave structures, satellite communication systems, holography, and alternative futures.

Professor Alexander is a registered Professional Engineer in the Province of Ontario and is active in community affairs.

Jianfen Liu received the B.Sc. degree Sichuan University (China) in July 1983 and Master of Science degree from Northwestern Polytechnical University in April 1986.

She worked as a lecturer in Nanjing Aeronautical Institute for three years after graduation. She is currently a Ph.D. candidate at the University of Windsor. Her main research area is gas discharges. She is a recipient of Post Graduate Award of Natural Sciences and Engineering Research Council of Canada.